Journal of Biomedical Optics

SPIEDigitalLibrary.org/jbo

Characterization of blood using terahertz waves

Kiyoung Jeong
Yong-Min Huh
Sang-Hoon Kim
Yeonji Park
Joo-Hiuk Son
Seung Jae Oh
Jin-Suck Suh

Characterization of blood using terahertz waves

Kiyoung Jeong,[a,b*] Yong-Min Huh,[b*] Sang-Hoon Kim,[b] Yeonji Park,[b] Joo-Hiuk Son,[c,] Seung Jae Oh,[b,] and Jin-Suck Suh[b,]
[a]Yonsei University, Graduate Program for Nanomedical Science, 50 Yonsei-ro, Seodaemun-gu, Seoul 120-749, Republic of Korea
[b]Yonsei University, YUHS-KRIBB Medical Convergence Research Institute, Severance Biomedical Science Institute, and Department of Radiology, 50 Yonsei-ro, Seodaemun-gu, Seoul 120-749, Republic of Korea
[c]University of Seoul, Department of Physics, 163 Siripdae-ro, Dondaemun-gu, Seoul 130-743, Republic of Korea

Abstract. We show that terahertz (THz) time-domain spectroscopy (TDS) can be used to characterize the blood. The complex optical constants of blood and its constituents, such as water, plasma, and red blood cells (RBCs), were obtained in the THz frequency region. The volume percentage of RBCs in blood was extracted and compared with the conventional RBC counter results. The THz absorption constants are shown to vary linearly with the RBC concentration in both normal saline and whole blood. The excellent linearity between the THz signal and the RBC concentration was also confirmed in a polyurethane resin tube using a THz imaging method. These results demonstrate that THz-TDS imaging can facilitate the quantitative analysis of blood. [DOI: 10.1117/1.JBO.18.10.107008]

Keywords: terahertz spectroscopy; terahertz imaging; blood spectroscopy; hematocrit; red blood cells; biomedical imaging.

Paper 130402R received Jun. 11, 2013; revised manuscript received Sep. 9, 2013; accepted for publication Oct. 1, 2013; published online Oct. 28, 2013.

1 Introduction

Recently, terahertz (THz) technology has attracted interest as an effective analysis method to characterize the molecular dynamics of biomaterials. This is because the majority of the conformational modes of water and biomolecules are contained in this frequency region.[1–7] The high sensitivity of THz waves allows diagnostic imaging of abnormal tissues, such as malignant tumors and burns, using differences in the concentrations of interstitial water or body fluid components in the tissues.[6–8] Studies of blood, tissue, and lymph fluids, as well as digestive juices, in the THz frequency range, therefore, have the potential to enhance the sensitivity of diagnostic images and expand the range of analyzable diseases.

Blood contains qualitative and quantitative information about essential substances and waste products in the body, and characterizing blood can facilitate early diagnosis of several diseases, including cancer.[9–12] For example, changes in the concentration of red blood cells (RBCs), which deliver oxygen and dioxide, can indicate the presence of anemia, blood cancer, or dengue fever. Various chemical, physical, and optical techniques have been exploited for blood analysis. Molecular information regarding, e.g., protein and nucleic acids in blood is acquired by molecular profiling methods, such as the western blot and the polymerase chain reaction.[13] Flow cytometry has also been employed to count and sort cells. However, these invasive and time-consuming methods require blood sampling.[13] Optical techniques, e.g., involving light-emitting diodes, have been used as noncontact, nondestructive analysis methods.[14] However, they are limited to analysis of blood in vessels just below the skin owing to the high scattering rate of visible light and the low penetration depth of mid-infrared light in tissues.

THz waves have a scattering rate lower than that of infrared and visible light and hence may be used as a feasible probe for analyzing blood inside vessels.[15] However, there are few reports of optical techniques utilizing the THz frequency range for blood characterization. In this study, we measured the optical constants of blood and its components using THz time-domain spectroscopy (TDS) and determined the correlation between the RBC concentration and the THz absorbance. These correlations are also present in a cylindrical tube containing blood with various RBC concentrations using THz imaging.

2 Materials and Methods

2.1 *THz Imaging System*

Two THz-TDS systems, operating in transmission and reflection mode, were established for the spectroscopy and spectroscopic imaging, respectively. Both systems used a mode-locked Ti:sapphire laser with 80-fs pulses at a central wavelength of 800 nm; the laser beam was split into two beams using a beam splitter. In the transmission mode system, one beam was focused onto a p-InAs wafer to generate THz pulses, whereas the other beam was focused onto a photoconductive antenna (PCA) fabricated on low-temperature-grown GaAs (LT-GaAs) to probe the THz pulses.[6] The THz waveforms were obtained via sampling of the cross-correlated signal between the optical probe pulse and the THz pulse at the detector using a slow-moving stage. The generated THz pulses were parallelized with a parabolic mirror and passed through the samples, which were placed between two parabolic mirrors. The transmitted THz pulses were guided to the detector using another parabolic mirror. The samples were placed in a liquid chamber composed of two z-cut

*These authors contributed equally to this work.

Address all correspondence to: Joo-Hiuk Son, University of Seoul, Department of Physics, 163 Siripdae-ro, Dondaemun-gu, Seoul 130-743, Republic of Korea. Tel: +82-2-2210-2607; E-mail: joohiuk@uos.ac.kr; Seung Jae Oh, Yonsei University, YUHS-KRIBB Medical Convergence Research Institute, Severance Biomedical Science Institute, and Department of Radiology, 50 Yonsei-ro, Seodaemun-gu, Seoul 120-749, Republic of Korea. Tel: +82-2-2228-7388; E-mail: issac@yuhs.ac; Jin-Suck Suh, Yonsei University, YUHS-KRIBB Medical Convergence Research Institute, Severance Biomedical Science Institute, and Department of Radiology, 50 Yonsei-ro, Seodaemun-gu, Seoul 120-749, Republic of Korea. Tel: +82-2-2228-7388; E-mail: jss@yuhs.ac

crystal-quartz windows, 3 mm in thickness, separated by a 100-μm Teflon spacer. The reflection mode THz system used a PCA that provided a +20 V bias to generate the THz pulses. These THz pulses were directed onto the sample by two parabolic mirrors, and the reflected pulses were guided to the LT-GaAs photoconductive detector using two other parabolic mirrors.[6] A fast delay line with an amplitude and frequency of 37 ps and 20 Hz, respectively, was used to obtain the THz pulses in real time. Both the spectroscopy and its imaging system were placed in chambers filled with dried air to eliminate the effects of water vapor. The samples were maintained at a temperature of 22°C (approximately room temperature). The signal-to-noise ratios of the transmission and reflection mode systems were 2300:1 and 1000:1, respectively, calculated from the peak-to-peak value of the pulses.

2.2 *Blood Sampling Method*

Blood was collected from the tail vein of three 9-week-old male Sprague-Dawley rats weighing ~400 g, and 0.1 μL heparin (Heparin-Natrium) was added per 1 mL blood to prevent clotting. The blood was centrifuged at 2000 rpm for 30 min to separate the plasma and the RBCs. We used 70-μL blood samples for the spectroscopy. The RBC concentration in the rat blood measured by the THz-TDS was compared to that obtained using a Hemavet R950 cell counter. We controlled the RBC concentration by diluting the RBCs in saline or plasma. This allowed us to reproduce the constituent concentration of some specific diseases. All experiments were conducted with the approval of the Association for Assessment and Accreditation of Laboratory Animal Care International.

3 Results and Discussion

The measured transmitted THz time-domain waveforms of blood and its ingredients are presented in Fig. 1(a). The THz waveforms of water with 0.1 μL heparin per 1 mL and saline containing 0.9% NaCl, both of which were used to dilute the samples, were almost identical to pure water. The amplitude of the pulse signal passing through the RBCs was the highest, followed by those of blood, plasma, and water, in descending order. Identical results were observed in the frequency domain waveforms obtained by the fast Fourier transform, as shown in Fig. 1(b).

The refractive index and absorption coefficients of the samples were obtained using the differences in amplitude and phase signals between the frequency domain signals with and without a sample, as shown in Fig. 2.[3] These constants decreased in the order of water, plasma, blood, and RBCs. The absorption coefficients of water, plasma, blood, and RBCs at 1 THz were 237.4, 231.1, 210.8, and 186.0 cm^{-1}, respectively. In other words, the absorbance of plasma, blood, and RBCs was 2.8%, 11.2%, and 21.6% lower than that of water, respectively. The differences could be explained by the different proportions of the water and biomaterials except water. The plasma, with an absorption coefficient close to that of water, was mainly water with only 8% of its composition being made up of various

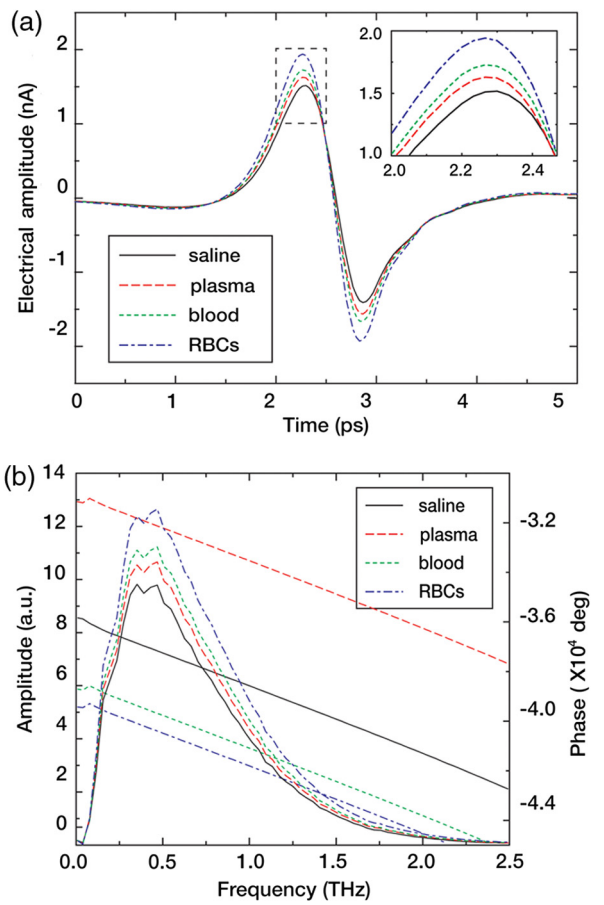

Fig. 1 Terahertz (THz) waveforms and complex optical constants of water, plasma, blood, and red blood cells (RBCs). (a) Time-domain waveforms and (b) frequency-domain waveforms from the same data.

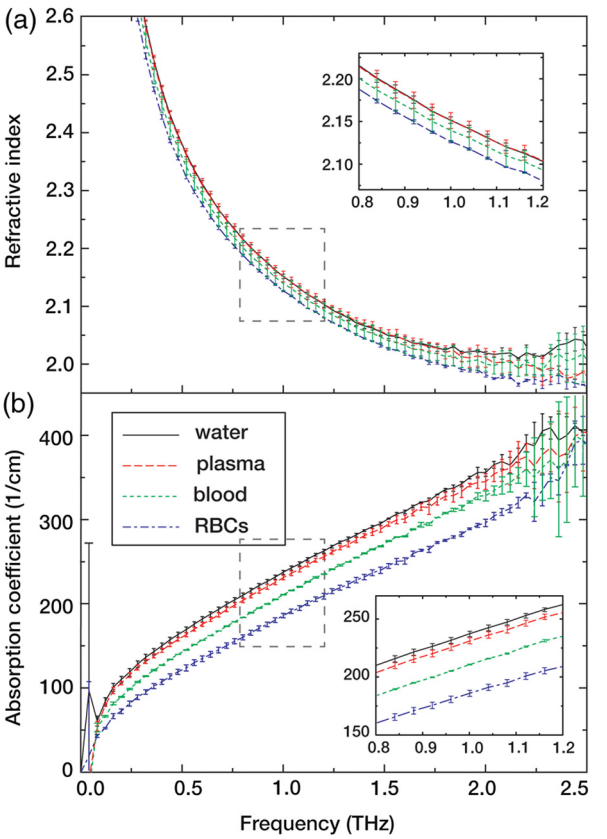

Fig. 2 THz complex optical constants of water, plasma, blood, and RBCs. (a) Refractive index and (b) absorption coefficients. The graphs in the insets show magnifications of the signal from 0.8 to 1.2 THz. The line and error bar represent the mean value and standard deviation of the optical constants of three blood samples, each obtained from a different rat.

Table 1 Comparison of volume fraction of red blood cells (RBCs).

Animal	V_{CBC} (%)	V_{THz} (%)	$\lvert V_{THz} - V_{CBC}\rvert$
A	46.13 ± 0.61	46.13 ± 2.79	0
B	48.87 ± 0.84	49.87 ± 3.94	1.11
C	49.37 ± 0.92	48.01 ± 3.59	1.36

proteins, fats, sugars, inorganic salt, urea, amino acids, and uric acid.[13] The RBCs had the smallest absorption coefficients, indicating that the water content of the RBCs was much lower than that of the plasma.

The absorption coefficient of the blood, which was composed mainly of RBCs and plasma, was in between those of plasma and RBCs as shown by the red line in Fig. 2(b). This implies that the absorbance of blood can be represented by a simple linear equation

$$\alpha_{\text{blood}} = V \cdot \alpha_{\text{RBCs}} + (1 - V) \cdot \alpha_{\text{plasma}}, \quad (1)$$

where α_{blood}, α_{RBCs}, and α_{plasma} are the absorption coefficients of blood, RBCs, and plasma and V indicates the volume fraction of the RBCs. As shown in Table 1, the volume fraction extracted by the THz technology corresponds to the volume fraction determined using a Hemavet R950 cell counter with an error of approximately <2%, even though the constituents beside RBCs and plasma, e.g., white blood cells and platelets which make up <1% of the blood, were disregarded. Hence, the hematocrit, which is the volume percentage of RBCs in blood, can be extracted using the THz spectroscopy.

To reveal the correlation between the hematocrit and the absorption coefficients in the THz region and THz sensitivity in the concentration of RBCs, we diluted the RBCs to various concentrations and measured the absorption coefficients of the samples. The RBCs were diluted in saline (0.9% NaCl) from 100% to 6.25% using the half-dilution method, which diluted one of two divided samples to a half concentration repeatedly. As shown in Fig. 3, as the concentration of RBCs decreased, the THz absorption coefficients increased. To show the quantitative relationship between the RBC concentration and the absorption coefficients, we extracted the absorption coefficients at 0.5, 1.0, and 1.5 THz as shown in Fig. 3(b). The relationship between the absorption coefficient and the RBC concentration was fitted well by linear equations ($R2 \approx 0.99$), indicating almost perfect

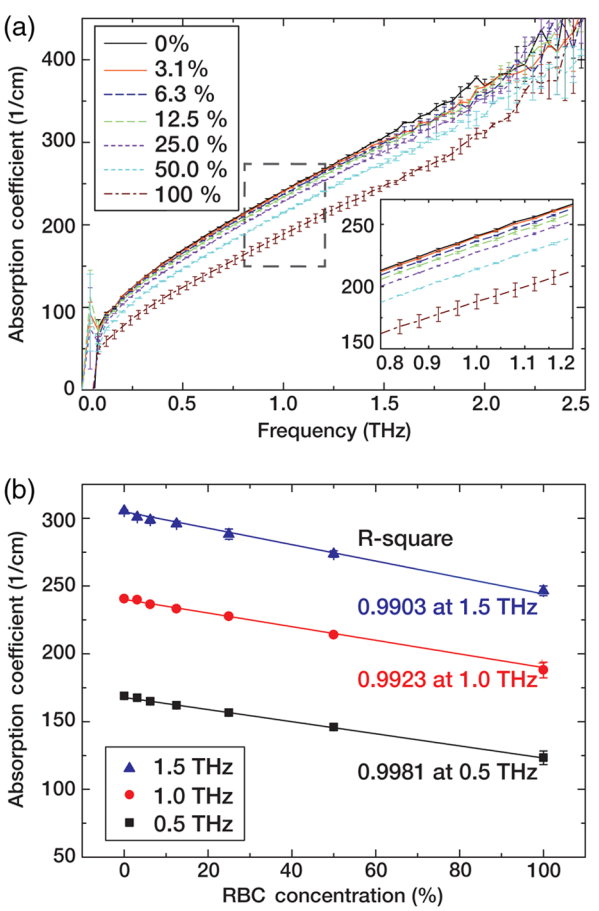

Fig. 3 Quantification of the RBC concentration in saline. (a) The absorption coefficients with varying RBC concentrations diluted in saline in the THz region. The graphs in the inset show a magnification of the signal from 0.8 to 1.2 THz. The lines and error bars represent the mean values and standard deviations of the optical constants of the three blood samples ($N = 3$). (b) The linear relation between the RBC concentration and the absorption coefficient at 0.5, 1.0, and 1.5 THz. The lines are linear fits at each frequency.

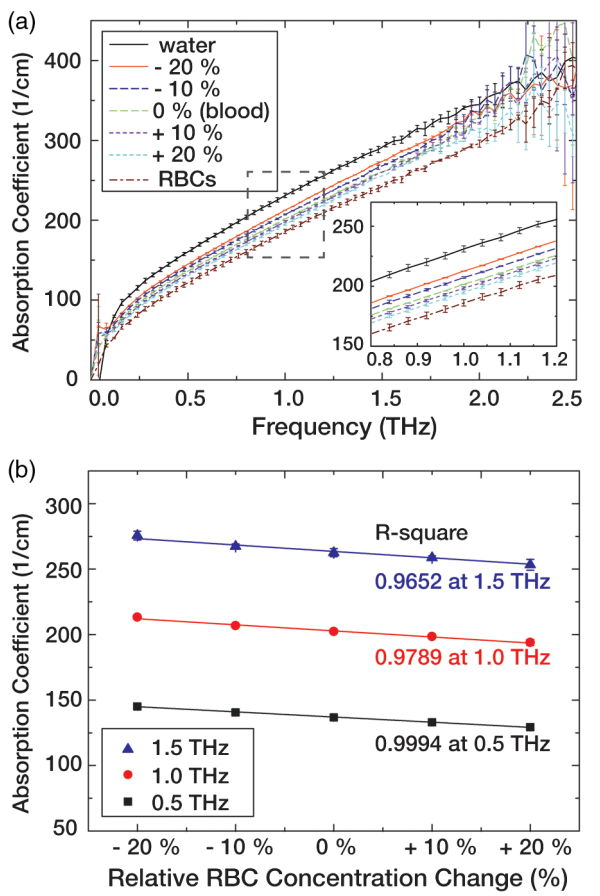

Fig. 4 Quantification of the RBC concentration in blood. (a) The absorption coefficients of various RBC concentrations. The added and eliminated volume rate are represented by the + and − symbols, ranging from +20 to −20. The graphs in the insets show magnifications of the signal from 0.8 to 1.2 THz. The lines and error bars represent the mean values and standard deviations of the optical constants of the three blood samples ($N = 3$). (b) The linear relationship between the relative RBC concentration change and the absorption coefficient at 0.5, 1.0, and 1.5 THz. The lines are linear fits at each frequency.

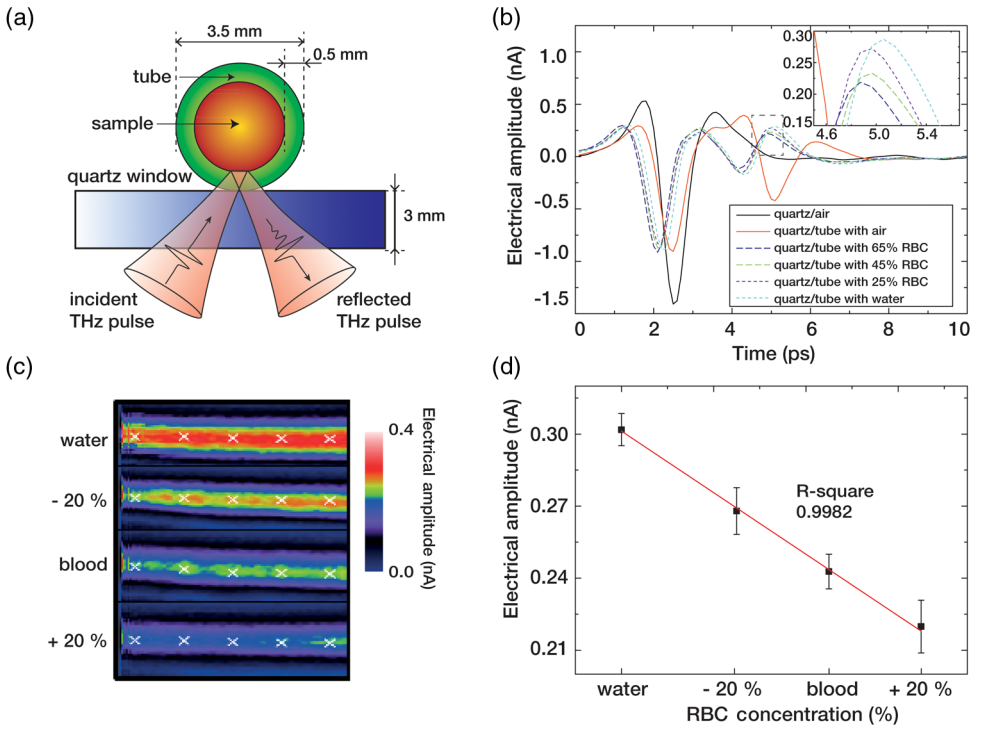

Fig. 5 THz images of the blood samples with various RBC concentrations in the cylindrical tube. (a) The THz imaging experiment scheme and the THz beam optical pathway on the sample. (b) Time-domain pulses reflected at the interface between the tube and the various samples. The graph in the inset shows expanded magnification of the signals between 4.5 and 5.7 ps. (c) Blood images of the blood vessel at the maximum points in the inset figure in (b). (d) The average values of contrast at the (*x*) marks in (c). The red solid line is a linear fit.

linearity with their sensitivity of ~3% RBC concentration. Thus, the hematocrit test can be performed by employing THz technology.

To demonstrate that the THz-hematocrit test can be realized clinically, the relation between the hematocrit and THz optical constants was verified in the blood. RBC-related diseases are generally suspected clinically when the RBC concentration is >70% or <30%.[13,14] Therefore, blood samples with various RBC concentrations were prepared by adding or eliminating RBCs with various concentrations and separated from the centrifuged blood. As the RBC concentration decreases, the THz absorption increases as shown in Fig. 4. The absorption coefficients at 0.5, 1.0, and 1.5 THz decrease linearly with increasing RBC concentration. The values fitted well with linear functions ($R^2 = 1.00$, 0.98, and 0.97, respectively), similar to the results in saline. The result confirms the feasibility of the hematocrit test in blood using THz waves.

Finally, we show that quantitative blood analysis imaging can be realized by THz imaging, using a cylindrical tube. Polyurethane resin tubes were positioned on a z-cut quartz window, as shown in Fig. 5(a). The tubes containing water and blood samples with RBC concentrations of 25%, 45%, and 65% were prepared. The time-domain signals were focused and reflected at different layers of the tube yielding the data presented in Fig. 5(b). The first (negative) peak of the pulse represents signals reflected at the interface between the quartz and the tube. The third (positive) peak (in the dashed box) indicates that the pulse was reflected at the interface between the tube and the samples in the tube. Thus, these third peaks include the optical properties of the samples and result in the image in Fig. 5(c).[5] As the RBC concentrations increase, the color scale of the images shifts from red to blue; these results are similar to the ones implemented above. To quantify the linearity of the images, we chose values at the 5 points indicated by (*x*) marks and extracted the means and standard deviations of these. These mean values show an excellent linear correlation of 0.9982 with the RBC concentrations, as shown in Fig. 5(d). This linear correlation confirms that quantitative blood analysis is feasible using THz spectroscopic imaging.

4 Conclusions

We have demonstrated that THz-TDS can be exploited as a quantitative blood analysis technique. The optical properties of blood and its ingredients, i.e., water, plasma, and RBCs, were characterized in the THz frequency range using a THz-TDS. The ratios of the optical constants of these components are identical to their volume fractions in nature. An excellent linear relationship between the THz absorbance and the RBC concentration was found in saline as well as in whole blood. Finally, we confirmed the feasibility of quantitative imaging of whole blood containing various concentrations of RBCs using the THz time-domain spectroscopic imaging system. This work has shown that THz imaging is potentially feasible for diagnosing blood-related diseases. In future work, we will extend our study to the noninvasive characterization of flowing blood.[16]

Acknowledgments

This study was supported by a grant from the Korean Health Technology Research and Development Project of the Ministry for Health, Welfare and Family Affairs, Republic of Korea (HI10C19110300) and National Research Foundation of Korea (NRF) grants funded by the Ministry of Education Science and Technology, Republic of Korea (2012R1A1A2008643, and 2012R1A2A2A01047402).

References

1. E. Pickwell and V. P. Wallace, "Biomedical applications of terahertz technology," *J. Phys. D: Appl. Phys.* **39**(17), R301–R310 (2006).
2. J.-H. Son, "Terahertz electromagnetic interactions with biological matter and their applications," *J. Appl. Phys.* **105**(10), 102033 (2009).
3. S. J. Oh et al., "Terahertz characteristics of electrolytes in aqueous Luria-Bertani media," *J. Appl. Phys.* **102**(7), 074702 (2007).
4. C. Ronne and S. R. Keiding, "Low frequency spectroscopy of liquid water using THz-time domain spectroscopy," *J. Mol. Liq.* **101**(1–3), 199–218 (2002).
5. P. U. Jepsen, J. K. Jensen, and U. Møller, "Characterization of aqueous alcohol solutions in bottles with THz reflection spectroscopy," *Opt. Express* **16**(13), 9318–9331 (2008).
6. S. J. Oh et al., "Molecular imaging with terahertz waves," *Opt. Express* **19**(5), 4009–4016 (2011).
7. J.-H. Son, "Principle and applications of terahertz molecular imaging," *Nanotechnology* **24**(21), 214001 (2013).
8. J. Fitzgerald et al., "Terahertz pulsed imaging of human breast tumors," *Radiology* **239**(2), 533–540 (2006).
9. H. Sloop, L. Dory, and P. S. Roheim, "Interstitial fluid lipoproteins," *J. Lipid Res.* **28**(3), 225–237 (1987).
10. P.-I. Hsu et al., "Diagnosis of gastric malignancy using gastric juice α1-antitrypsin," *Cancer Epidemiol. Biomarkers Prev.* **19**(2), 405–411 (2010).
11. S. Nagrath et al., "Isolation of rare circulating tumour cells in cancer patients by microchip technology," *Nature* **450**(7173), 1235–1239 (2007).
12. E. A. Punnoose1 et al., "Molecular biomarker analyses using circulating tumor cells," *PLoS One* **5**(9), e12517 (2010).
13. B. F. Rodak, G. A. Fritsma, and K. Doig, Chapters 6 & 14 in *Hematology: Clinical Principles and Applications*, Elsevier Health Sciences, Atlanta, Georgia (2007).
14. M. C. P. van Beekvelt et al., "Performance of near-infrared spectroscopy in measuring local O2 consumption and blood flow in skeletal muscle," *J. Appl. Physiol.* **90**(2), 511–519 (2001).
15. P. Y. Han, G. C. Cho, and X.-C. Zhang, "Time-domain transillumination of biological tissues with terahertz pulses," *Opt. Lett.* **25**(4), 242–244 (2000).
16. S. J. Oh et al., "Measurement depth enhancement in terahertz imaging of biological tissues," *Opt. Express* **21**(18), 21299–21305 (2013).